

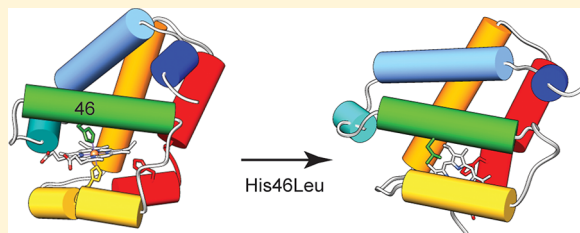
Replacement of the Distal Histidine Reveals a Noncanonical Heme Binding Site in a 2-on-2 Hemoglobin

Dillon B. Nye and Juliette T. J. Lecomte*

T. C. Jenkins Department of Biophysics, Johns Hopkins University, Baltimore, Maryland 21218, United States

 Supporting Information

ABSTRACT: Heme ligation in hemoglobin is typically assumed by the “proximal” histidine. Hydrophobic contacts, ionic interactions, and the ligation bond secure the heme between two α -helices denoted E and F. Across the hemoglobin superfamily, several proteins also use a “distal” histidine, making the native state a bis-histidine complex. The group 1 truncated hemoglobin from *Synechocystis* sp. PCC 6803, GlbN, is one such bis-histidine protein. Ferric GlbN, in which the distal histidine (His46 or E10) has been replaced with a leucine, though expected to bind a water molecule and yield a high-spin iron complex at neutral pH, has low-spin spectral properties. Here, we applied nuclear magnetic resonance and electronic absorption spectroscopic methods to GlbN modified with heme and amino acid replacements to identify the distal ligand in H46L GlbN. We found that His117, a residue located in the C-terminal portion of the protein and on the proximal side of the heme, is responsible for the formation of an alternative bis-histidine complex. Simultaneous coordination by His70 and His117 situates the heme in a binding site different from the canonical site. This new holo protein form is achieved with only local conformational changes. Heme affinity in the alternative site is weaker than in the normal site, likely because of strained coordination and a reduced number of specific heme–protein interactions. The observation of an unconventional heme binding site has important implications for the interpretation of mutagenesis results and globin homology modeling.



Steady improvement in genome sequencing has provided structural biologists with an enormous number of new sequences across all superfamilies of proteins. Hemoglobins (Hbs) are no exception to this sudden increase in the amount of information. Thousands of hypothetical globin genes are now available with multiple representatives in nearly all forms of life. Traditionally viewed as oxygen transporters, Hbs assume other functions related to the management of small molecules, principally reactive oxygen and nitrogen species.^{1–3} These other functions are emphasized in unicellular organisms under aerobic and anaerobic conditions. Unlike for proteins devoid of cofactors, however, functional prediction in globins and rational design based on the globin fold are complicated by the exquisite sensitivity of the reactive heme group to small variations in structure. To this day, it is a challenge to anticipate such a fundamental property as protein ligands to the iron given a primary structure unequivocally corresponding to a globin. Without clear determinants of heme ligation and consequently reactivity, the wealth of information contained in expanding sequence databases cannot be fully exploited.

In efforts to explore and rationalize the natural range of chemistry supported by the Hb scaffold, we and others have used GlbN, the monomeric Hb from the cyanobacterium *Synechocystis* sp. PCC 6803, as a model protein.^{4–6} GlbN is a representative of the “truncated” lineage of the superfamily; as such, it is several residues shorter than mammalian myoglobins but preserves essential structural features of the globin fold: the B, E, G, and H helices assemble in an orthogonal bundle and form a hydrophobic core, while the *b* heme group is captive

between the E and F helices. The F helix provides the strictly conserved proximal His70 (F8 in myoglobin notation) as an axial ligand to the heme iron. In GlbN, a second axial ligand, His46 (E10), is found on the opposite (distal) side of the heme.⁷ Bis-histidine ligation classifies GlbN as a “hexacoordinate” globin, so-called because the heme iron is coordinated by two protein side chains as well as the four pyrrole nitrogens of the porphyrin.

Endogenous hexacoordination is observed in many globins throughout the superfamily, as a native property,⁸ a stable misfolded state,⁹ or a species appearing transiently during folding processes.^{10,11} As a native state property, bis-histidine ligation tunes the iron reduction potential, establishes activation energy barriers for substrate binding, and determines the propensity for various types of reactions. For these reasons, the attributes that allow a distal histidine to serve as a ligand and the attributes that prevent a distal histidine from serving as a ligand have been a focus of investigation.¹² The difference between GlbN and myoglobin, which uses only the proximal histidine as an axial ligand in the native state, highlights the importance of scaffold rigidity and the need for a description of the conformational space accessible to various globins.

GlbN is an excellent subject for studying the role and extent of plasticity in the globin fold. Figure 1 illustrates the bis-histidine

Received: July 14, 2018

Revised: September 12, 2018

Published: September 14, 2018

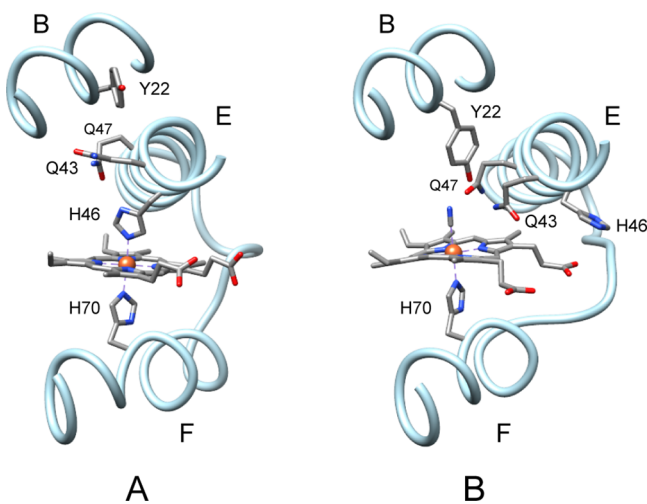


Figure 1. Residues of interest in the heme binding site of GlbN (A) in the bis-histidine state (PDB entry 1RTX)¹³ and (B) in the cyanomet state (PDB entry 1S69).¹⁴ The E and F helices are shown, along with a portion of the B helix.

structure¹³ and the changes occurring when His46 is displaced by an exogenous ligand, cyanide in this case.¹⁴ A trio of residues, Tyr22 (B10), Gln43 (E7), and Gln47 (E11), is introduced into the distal pocket to form a hydrogen bond network with bound cyanide. When using the coordinate transformation matrix minimizing the overall $C\alpha$ rmsd between the two structures, displacements are systematically >2 Å in the A and E helices and the beginning of the B helix. Gly63, which initiates the F helix in the bis-histidine structure, moves by >11 Å. Overall, helices rotate and translate as rigid objects while remaining nearly intact. Loops and turns, endowed with some conformational freedom, are key to the rearrangement.

The question of whether structural strains are imposed in the bis-histidine state or in the exogenously coordinated state has been investigated with studies of wild-type (WT) GlbN,⁵ Zn-substituted GlbN,¹⁵ and His46 variants.^{12,14} For the distal variant proteins, a reasonable expectation is that, via elimination of an axial ligand, the structure will relax and the iron will assume a high-spin character, as a pentacoordinate complex (ferrous state, $S = 2$, or ferric state, $S = 5/2$) or a water-bound hexacoordinate complex (ferric state, aquomet, $S = 5/2$). Electronic absorption, electron paramagnetic resonance (EPR), and nuclear magnetic resonance (NMR) studies of ferric H46A and H46L GlbN, however, do not fulfill this expectation. Ferric H46L is almost entirely low-spin ($S = 1/2$),¹⁶ whereas H46A is a mixture of a low-spin and an aquomet high-spin complex.^{7,16} Ferrous H46A and H46L GlbN also show a degree of low-spin ($S = 0$) character by electronic absorption spectroscopy or EPR.^{5,7,16} Because these observations are made in the absence of exogenous ligand, the coordination status of the His46 variants betrays an unusual behavior and merits elucidation.

The structural rearrangement shown in Figure 1 suggests that any of the residues forming the hydrogen bond network in the cyanomet complex may be able to reach the iron in the H46L variant. These candidates were tested with puzzling results. Y22F/H46L GlbN displays NMR signatures of an unchanged ferric complex compared to H46L GlbN,¹⁶ and the Q43L/H46L replacement does not eliminate fully the low-spin properties of the ferrous state.⁵ Inspection of the bis-histidine and cyanide-bound structures leaves as possibilities Gln47 and other less obvious candidates. In this work, our goal was to

identify the alternative distal ligand(s) in H46L GlbN to document the plasticity of the GlbN fold. We resorted to mutagenesis and the use of a modified heme in NMR spectroscopy studies to analyze the distorted GlbN structure. We show that a single-amino acid replacement can lead to a profound perturbation of the heme–protein topology without extensive alteration of the polypeptide fold. The results contribute to an improved understanding of the role of protein flexibility in limiting the properties of globins and emphasize the need for systematic experimental characterization of newly discovered globin sequences.

MATERIALS AND METHODS

Protein Purification. Variant GlbN proteins were overexpressed in *Escherichia coli* BL21 cells using a pET3c plasmid vector. H46L and H46L/Q47L apoGlbNs partitioned primarily into the cell lysate, as opposed to inclusion bodies, and were purified according to published procedures.^{16,17} Porcine hemin chloride (Sigma, 20 mg/mL in 0.1 M NaOH) was added to the crude lysate until full holoprotein reconstitution was observed by electronic absorption spectroscopy.¹⁶ This procedure produced a variable amount of ferrous O_2 -bound complex, and 1 mM $K_3[Fe(CN)_6]$ was added to ensure a homogeneous ferric product. The holoprotein was then purified by size exclusion and anion exchange chromatography. For the H46L/H117A GlbN variant, the apoprotein was purified directly from the cell lysate by size exclusion and anion exchange chromatography. Hemin chloride was added to reconstitute the holoprotein, which was separated from excess hemin by an additional round of size exclusion chromatography. Purity was assessed by sodium dodecyl sulfate–polyacrylamide gel electrophoresis and mass spectrometry. The typical yield was 100 mg/L. Uniformly ^{15}N -labeled or ^{15}N - and ^{13}C -labeled protein was purified in the same manner from cells grown in M9 minimal medium containing $^{15}NH_4Cl$ and $[^{13}C]glucose$ as the sole sources of nitrogen and carbon, respectively. Following the final chromatography step, purified holoproteins were exchanged into storage buffer [0.5 mM Na/K phosphate (pH 7)], lyophilized, and stored at -20 °C.

Reconstitution with Mesoheme. Purified H46L and H46L/Q47L GlbN holoproteins were converted to their apoprotein forms using the procedure of Teale.¹⁸ Fe(III) mesoporphyrin IX chloride (mesoheme, Frontier Scientific, 5–10 mg/mL in 0.1 M NaOH) was added in an \sim 2-fold molar excess to the stirred apoprotein solution [200 μ M GlbN and 20 mM Na/K phosphate (pH 7.2), 5–10 mL], and the reconstitution reaction was allowed to proceed for several hours at 4 °C. The modified holoprotein was separated from excess mesoheme by anion exchange chromatography, exchanged into storage buffer, and lyophilized if not immediately used.

Electronic Absorption Spectrophotometry. Electronic absorption spectra were recorded using a Cary50 ultraviolet–visible spectrophotometer. Spectra of ferric complexes were recorded from 800 to 260 nm in 1 nm steps using a 0.1 s averaging time. Ferrous deoxy samples were generated by addition of 2 mM sodium dithionite (DT, Alfa Aesar), and spectra were recorded from 650 to 350 nm every 1 min. pH titrations were performed in 5 mM Na/K phosphate as reported previously.¹⁹ Concentrations were determined on a per heme basis using extinction coefficients obtained by the pyridine (SigmaAldrich) hemochromogen assay.^{20,21}

Circular Dichroism. Circular dichroism (CD) spectra of GlbN variants [15 μ M, 25 mM Na phosphate (pH 7.4–7.5)]

were recorded using an Aviv model 420 spectropolarimeter. Far-ultraviolet (far-UV) spectra were recorded with a 1 mm path length cuvette over the range of 300–190 nm in 1 nm steps using a 3 s averaging time. Soret CD spectra were recorded on the same sample over the range of 500–300 nm using a 1 cm path length cuvette. The sample temperature was maintained at 25 °C.

Heme Transfer Kinetics. Horse myoglobin (Mb, Sigma) was converted to the apoprotein state by the procedure of Teale, as described above, and further purified using a 100 cm \times 2.5 cm G-50 (Sigma) size exclusion column. Concentrations of apoMb were determined using the calculated extinction coefficient of 13980 M⁻¹ cm⁻¹ at 280 nm.²² ApoMb was added to a ferric H46L GlbN sample [5 or 10 μ M, 100 mM Na phosphate (pH 7.2)], and absorbance spectra were recorded in intervals of 70 s for 2 h. The reaction kinetics were found to be independent of H46L GlbN and apoMb concentrations (above a 2.5-fold molar excess of apoMb). Singular-value decomposition was applied to kinetic data sets, and two abstract vectors were globally fit to a single exponential using Mathematica (Wolfram Research, Champaign, IL). The apparent first-order rate constant is taken to represent the heme k_{off} .²³ In a similar experiment, the addition of apoMb was immediately followed by the addition of 2 mM DT.

Heme Cross-Linking in H46L/Q47L GlbN. GlbN is capable of spontaneously forming a covalent linkage between His117 Nε2 and the heme 2-vinyl C α atom in the bis-histidine ferrous state.²⁴ The linkage is made rapidly ($k \sim 0.4$ s⁻¹ at pH 7²⁵) by the addition of DT to the recombinant ferric protein. H46L GlbN is less reactive, but aided by added imidazole or cyanide.¹⁶ On the basis of these results, the covalent linkage was generated in samples of H46L/Q47L GlbN [1–5 mM, 100 mM Na/K phosphate (pH 7–7.5)] by overnight incubation with 2–5 mM DT, followed by oxidation using 5 mM K₃[Fe(CN)₆] and passage over a 1 cm \times 50 cm G-25 (Sigma) desalting column equilibrated in 10 mM Na/K phosphate (pH 7). Formation of the cross-link was verified by mass spectrometry and comparison to previously published NMR data.¹⁶

NMR Spectroscopy. NMR spectra were recorded at a field strength of 14.1 T using a Bruker Avance or Avance II spectrometer, each equipped with a TXI cryoprobe, or at a field strength of 18.8 T using a Varian INOVA spectrometer. ¹H chemical shifts were referenced indirectly through the residual water signal. ¹⁵N and ¹³C chemical shifts were referenced indirectly using the Ξ ratios.²⁶ Topspin 3.1 was used to process and analyze 1D data. Multidimensional data sets were processed with NMRPipe 3.0²⁷ and analyzed with Sparky3.²⁸ Select 3D correlation experiments were acquired using a Poisson-Gap sampling schedule in both indirect dimensions.²⁹ Non-uniformly sampled spectra were reconstructed using the NESTA-NMR software package implemented on the NMRbox virtual machine.^{30,31}

Mesoheme ¹H assignments for ferric H46L mesoGlbN [0.5 mM, 20 mM Na/K phosphate (pH* 7.3), 99% ²H₂O] and ferric H46L/Q47L mesoGlbN [2 mM, 30 mM Na/K phosphate (pH* 7.2), 99% ²H₂O] were achieved using standard homonuclear experiments (NOESY, WEFT-NOESY, DQF-COSY, and TOCSY). ¹H nonselective spin–lattice relaxation times (T_1) were determined with a simple inversion recovery sequence. ¹H, ¹⁵N, and ¹³C assignments of H46L/Q47L GlbN [2 mM, 25 mM Na phosphate (pH 7.2), 5% ²H₂O] and H46L/Q47L mesoGlbN [2.5 mM, 20 mM Na phosphate (pH 7.1), 5% ²H₂O] were obtained using ¹H–¹⁵N HSQC,

¹H–¹³C HSQC, ¹H–¹⁵N–¹H TOCSY-HSQC³² ($\tau_{\text{mix}} = 45$ ms), HNCO,³³ CBCA(CO)NH,³⁴ HNCACB,³⁵ HBHA(CO)NH,³⁴ and C(CO)NH³⁶ and H(CCO)NH³⁶ ($\tau_{\text{mix}} = 15$ ms) experiments. Amide NOEs were measured with ¹H–¹⁵N–¹H NOESY-HSQC³² spectra ($\tau_{\text{mix}} = 80$ ms), and ¹³CH₃ selective ¹H–¹³C HSQC and ¹H–¹³C–¹H NOESY-HSQC³⁷ spectra ($\tau_{\text{mix}} = 70$ ms) were recorded on H46L/Q47L mesoGlbN exchanged into 99% ²H₂O.

RESULTS

Ruling Out Gln47 and Hydroxide Ligation. The residues composing the hydrogen bond network of cyanomet GlbN (Figure 1B) are not far from the iron and could coordinate in the H46L variant with a modest distortion of the 3D structure. To complement prior work on Y22F/H46L GlbN¹⁶ and Q43L/H46L GlbN,⁵ H46L/Q47L GlbN was prepared and compared to H46L GlbN. The electronic absorption spectra of the single and double variants at neutral pH (Figure 2) are nearly identical to one another, each

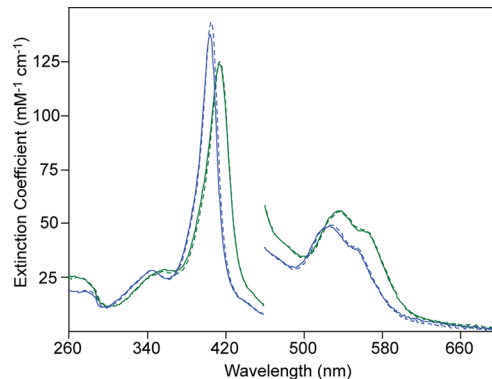


Figure 2. Electronic absorption spectra of ferric GlbN variants containing mesoheme (blue) or *b* heme (green) at neutral pH. H46L GlbN (solid lines) and H46L/Q47L GlbN (dashed lines) are shown.

displaying a Soret peak at 414 nm and lacking the long-wavelength charge transfer band of a high-spin complex. In the NMR spectra, hyperfine-shifted ¹H signals are observed in the 30 to –20 ppm window only (Figure 3A,B). Nonselective T_1 values were determined for peaks tentatively assigned to the heme methyl groups (Figure S1) and found to be \sim 65 ms at the shortest. Both ¹H shifts and T_1 values are consistent with a principally low-spin iron.³⁸ Thus, in the absence of additional ligand switching, the set of Tyr22, Gln43, and Gln47 variants rejects these residues from contention.

A structurally conservative interpretation of the ferric low-spin H46L GlbN data implicates hydroxide ions. His–Fe–OH[–] complexes exist in low-spin/high-spin equilibria with a low-spin ground state.³⁸ The pK_a of the transition between hydroxymet and aquomet species varies, with values generally above 7.^{39,40} Stabilization of the hydroxymet state over the high-spin aquomet state at neutral pH is occasionally observed, M80A iso-1-cytochrome *c* providing one example.^{41,42} The pH titration of H46L GlbN monitored by electronic absorption spectroscopy¹⁶ shows that the onset of the transition to an aquomet species occurs below pH 5, suggesting that, if hydroxide is the ligand, it is highly stabilized by the protein structure. Such enhanced stabilization of the hydroxymet species could be accomplished by hydrogen bond donation by Tyr22, as in the cyanomet complex, assisted by Gln43 and Gln47.

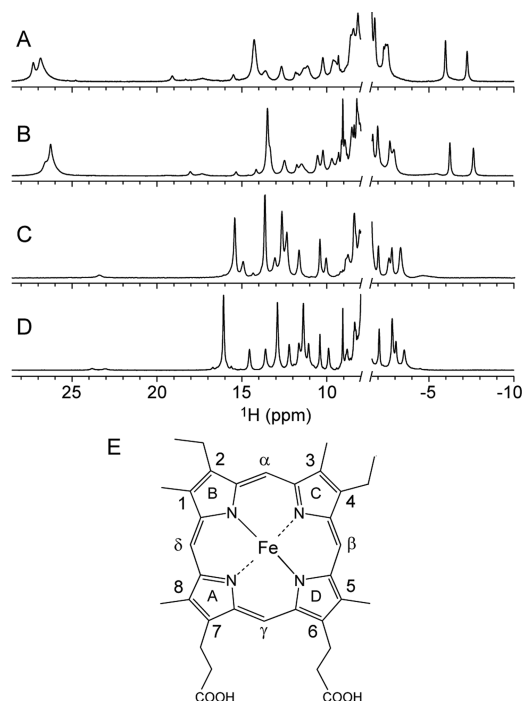


Figure 3. ^1H NMR spectra of ferric (A) H46L GlbN,¹⁶ (B) H46L/Q47L GlbN, (C) H46L mesoGlbN, and (D) H46L/Q47L mesoGlbN. All samples contain 99% $^2\text{H}_2\text{O}$ at pH^* 7.0–7.5. The vertical scaling is arbitrary. The *b* heme spectra (A and B) display a pair of broad peaks near -15 ppm that are not shown. (E) Structure of mesoheme and the nomenclature used in the text. Heme *b* has vinyl groups at positions 2 and 4.

However, the Y22F¹⁶ and Q47L (Figure S2A) replacements in the H46L background do not change the pH response compared to that of H46L GlbN. If hydroxide coordination is indeed the source of the low-spin complex, some other stabilization mechanism must be at work.

The apparent pK_a of the coordinated water molecule depends in part on the heme electronic structure.^{39,43} Replacement of the *b* heme in Mb with mesoheme (Figure 3E) increases the apparent pK_a by ~ 0.5 unit by increasing the electron density at the iron.^{40,44} To test the hypothesis of a hydroxide ligand further, the H46L and H46L/Q47L variants of GlbN were prepared with mesoheme. The electronic absorption spectra of H46L and H46L/Q47L mesoGlbN (Figure 2) match those of the parent proteins, after accounting for a 10 nm hypsochromic shift caused by a decrease in the extent of heme conjugation. The low-pH dependence of the electronic absorption spectra of H46L/Q47L mesoGlbN is similar to that of the heme *b* complex, showing protein denaturation and heme release with an apparent pK_a of ~ 4 (Figure S2B). Decoupling of ligand protonation and acid denaturation is not observed, so that the pK_a of a bound hydroxide would have to be remarkably low to explain the result. The NMR relaxation and shift data also suggest a thermally inaccessible high-spin state. An isotope effect on chemical shift, expected in the event of strong hydrogen bonding,⁴⁵ is absent upon comparison of spectra recorded in H_2O and $^2\text{H}_2\text{O}$ (not shown), which weakens this hydroxide hypothesis further. The alternative to hydroxide binding is that one strong-field ligand is provided by the protein. At the simplest, the same protein residue would coordinate the iron in the ferric and ferrous states.

Identification of the Heme Ligands in H46L GlbN. The ^1H NMR spectra of H46L mesoGlbN and H46L/Q47L mesoGlbN are shown in Figure 3. Reduced dispersion relative to the *b* heme counterparts is attributed to an increase in electronic distribution symmetry^{46,47} and a possible alteration of the axial ligand orientation.⁴⁸ From a spectral analysis perspective, the loss of dispersion in mesoGlbN is compensated by sharpened resonances, and of H46L mesoGlbN and H46L/Q47L mesoGlbN, the double variant presented higher-quality data. This protein was therefore chosen for further study. Mesoheme assignments (Table S1) were achieved using 2D homonuclear data. Resolved mesoheme methyl resonances have T_1 values between 80 and 120 ms (Figure S1 and Table S1), shorter than those of *b* heme in WT GlbN (130–260 ms),¹⁷ but nevertheless consistent with a low-spin iron.⁴⁹ Fast-relaxing nuclei belonging to the protein were also detected in 1D data as shown in Figure 4. For a ferric $S = \frac{1}{2}$ porphyrin complex, if

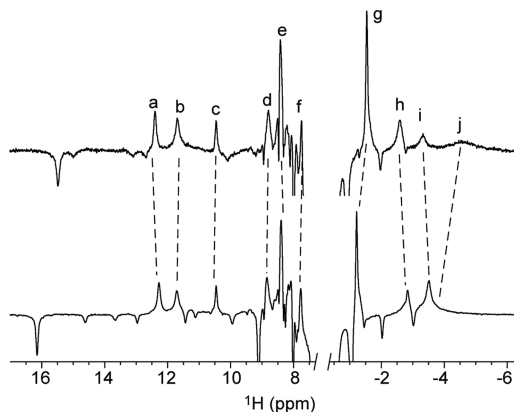


Figure 4. ^1H NMR inversion recovery spectra of H46L mesoGlbN (top, 0.5 mM, 99% $^2\text{H}_2\text{O}$, pH^* 7.3) and H46L/Q47L mesoGlbN (bottom, 2 mM, 99% $^2\text{H}_2\text{O}$, pH^* 7.2) using a 50 ms recovery delay. Positive peaks identify protons within ~ 6 Å of the ferric iron: (a) His70 $\text{H}^{\beta 3}$, (b) His117 $\text{H}^{\beta 3}$, (c) Phe84 H^{α} , (d) mesoheme δ -meso, (e) Phe84 $\text{H}^{\epsilon 1/\epsilon 2}$, (f) His117 H^{α} , (g) Val74 $\text{H}^{\gamma 1}$, (h) mesoheme α -meso H , (i) mesoheme γ -meso H , and (j) unassigned.

spin delocalization is neglected, the T_1 of protons near the paramagnetic center is dominated by the dipolar mechanism with R^6 dependence on the distance from the iron.⁵⁰ Crude distance estimates situate these protons within 6 Å of the iron, a distance appropriate for heme ligands.

To identify the fast-relaxing protons, H46L/Q47L apoGlbN was uniformly labeled with ^{15}N and ^{13}C and reconstituted with mesoheme. The ^1H – ^{15}N HSQC spectrum of the resulting complex is shown in Figure S3 to illustrate data quality. Unambiguous sequential assignments from Leu4 to Gln124 (except prolines) were achieved with 3D triple-resonance experiments. Assignments for selected residues are listed in Table S2. Of note is the $^{68}\text{EAHKE}$ string of shifted signals, which identifies His70. This residue has one efficiently relaxed $\text{C}\beta\text{H}$ proton, and the $^{13}\text{C}^\alpha$ and $^{13}\text{C}^\beta$ signals are significantly shifted from the mean diamagnetic value for this type of residue (Table 1). The spectral characteristics of His70 condition expectations for the resonances of the distal ligand. Indeed, a second set of signals with shifts and relaxation properties similar to those of His70 is detected, embedded in the $^{116}\text{AHKR}$ sequence (Figure 5 and Table 1): we conclude that His117 is the distal ligand in H46L/Q47L mesoGlbN. ^1H assignments for His70 and His117 were readily transferred to

Table 1. Selected ^1H Chemical Shifts and T_1 Values in H46L/Q47L GlbN and H46L/Q47L GlbN MesoGlbN^a

residue	nucleus	mesoH46L/Q47L		H46L/Q47L	
		δ (ppm)	T_1 (ms)	δ (ppm)	T_1 (ms)
His70	NH	10.39		10.35	
	H^α	7.97		7.80	
	$\text{H}^{\beta 3}$	12.32	45	12.55	35
	$\text{H}^{\beta 2}$	8.02		8.10	
	N	120.1		119.8	
	C^α	82.9		84.8	
	C^β	22.5		22.2	
His117	NH	11.49		11.23	
	H^α	7.78	60	7.49	
	$\text{H}^{\beta 3}$	11.70	50	11.56	35
	$\text{H}^{\beta 2}$	8.18		8.39	
	N	119.6		119.2	
	C^α	73.7		74.2	
	C^β	20.9		N.D.	

^aAt 25 °C, 5% $^2\text{H}_2\text{O}$, and pH 7.1. T_1 values have a standard error of <5% (Figure S1).

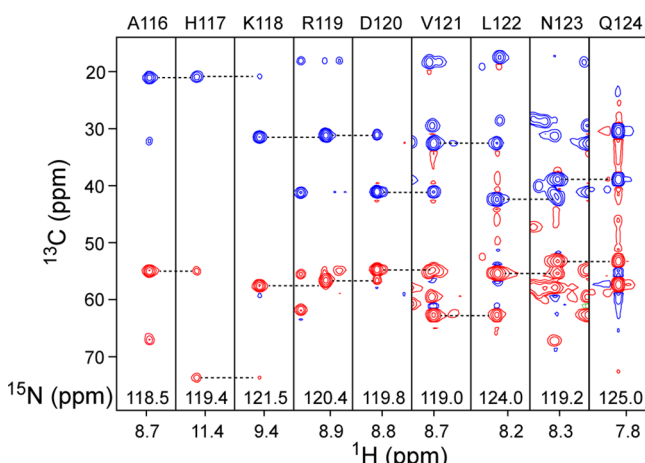


Figure 5. Portion of the HNCACB spectrum of H46L/Q47L mesoGlbN [2.5 mM GlbN, 20 mM Na phosphate (pH 7.1), 5% $^2\text{H}_2\text{O}$]. An isolated string of nine residues was observed and assigned to A116–Q124, the C-terminal stretch preceded by P115. The plane labeled H117 is amplified 2-fold.

the H46L variant, confirming that the Q47L replacement had no influence on the identity of the axial ligands.

If His117 is a ligand, ferric H46L/H117A GlbN is expected to bind the heme with the proximal histidine and form an aquomet (or hydroxymet) complex, as long as no further distortion of the fold and no additional ligand switching occurs. The ^1H NMR spectrum of the double variant acquired at neutral pH (Figure S4A) is consistent with a predominantly aquomet species (hyperfine shifts of >60 ppm). The electronic absorption spectra agree and, as the pH is increased, reveal an aquomet to hydroxymet transition with an apparent pK_a of ~8.6 (Figure S4B). In the ferrous state, the H117A replacement eliminates the spectral features of endogenous hexacoordination observed in H46L GlbN (Figure 6). These results are consistent with His117 being a heme ligand in the ferric and ferrous oxidation states of H46L (meso)GlbN. In what follows, we refer to the conformation of the holoprotein with His70–Fe–His117 ligation as GlbN*.

Effects of Heme Substitution in H46L/Q47L GlbN.

Hyperfine ^1H chemical shifts are highly sensitive to the nature

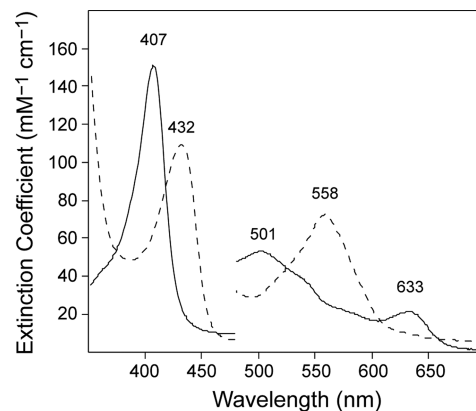


Figure 6. Electronic absorption spectra of H46L/H117A GlbN at neutral pH. The ferric aquomet state (solid line) was converted to the ferrous deoxy state (dashed line) by addition of DT. The visible regions of the spectra have been amplified 5-fold.

of the heme ligation (ligand identity, geometry, H-bonding, etc.). Comparison of data collected on GlbN* and mesoGlbN* reveals that the heme substitution in the H46L or H46L/Q47L variants does not alter the His70/His117 scheme (Table 1). However, the ^1H – ^{15}N HSQC spectrum of H46L/Q47L GlbN* (Figure S5) shows two forms in an ~8:2 ratio, whereas the H46L/Q47L mesoGlbN* counterpart displays only one form. The population of two holoprotein forms conserving the same ligand set but accommodating the heme in two orientations related by an ~180° rotation about the α – γ meso axis is commonly observed in heme proteins.³⁸ This “heme rotational isomerism” has modest structural consequences and is modulated by both direct and remote heme–protein interactions.^{51–53} The small differences in ^1H – ^{15}N chemical shifts between the major and minor forms of H46L/Q47L GlbN* (Figure S6A) support the idea that this heme rotational heterogeneity is the origin of NMR signal duplication.⁵⁴ Backbone amide assignments for the major heme *b* isomer closely match those of the mesoheme complex (Figure S6B). To a first approximation, structural information available from the high-quality NMR spectra of H46L/Q47L mesoGlbN* holds for both the major isomer of the heme *b* complex and the H46L single variant. As expected because of changes in structure and in the paramagnetic susceptibility tensor, large chemical shift differences are observed between WT GlbN and H46L/Q47L GlbN* (Figure S6C).

Structural Properties of GlbN*. The NMR model of WT GlbN (PDB entry 1MWB)⁵⁵ shows that His117 is positioned on the same face of the heme as the proximal histidine and points toward the heme in some conformers or away from it in others. Evidence of axial iron ligation by His70 and His117 in GlbN* implies not only a displacement of the heme but also inevitably some structural reorganization of the protein. Circular dichroism was used to assess secondary structure perturbation. The far-UV CD spectra (Figure 7A) of GlbN*, with heme *b* or mesoheme, display signatures of high α -helical content consistent with expectations informed by the WT structure.⁴ Larger differences are observed in the visible region of the spectrum (Figure 7B). In contrast to the negative Soret CD band of WT GlbN,⁴ the double variants display positive Soret peaks, which may be related to different interactions with aromatic side chains and conformations of the heme propionates.⁵⁶

CD data show a similar helical content of GlbN and GlbN* but offer limited insight into the structural changes that

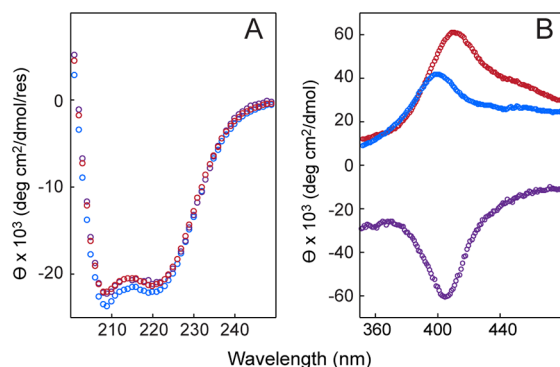


Figure 7. Circular dichroism spectra of WT GlbN (purple, 15 μ M, pH 7.4), H46L/Q47L GlbN* (red, 15 μ M, pH 7.4), and H46L/Q47L mesoGlbN* (blue, 15 μ M, pH 7.5): (A) far-UV region and (B) Soret region.

accommodate the unusual ligation scheme. To identify residue-specific distortions in secondary structure associated with His117 coordination, TALOS+ analysis⁵⁷ was applied to backbone ¹H, ¹³C, and ¹⁵N chemical shifts of H46L/Q47L mesoGlbN* and WT GlbN (Figure 8). TALOS+ secondary structure predictions are supported by the detection of helical NOEs in the variant (diagrammed in Figure S7) and the WT protein.⁵⁸ There is substantial agreement between GlbN and GlbN* and between GlbN and its solution structure. Exceptions include residues 32–35, which TALOS+ classifies as a loop in GlbN but which actually form the β -helix in solution both in WT GlbN⁵⁸ and in GlbN*, and residues in the vicinity of His117. Distortion of this region is an expected consequence of heme ligation by His117. Predicted order parameters, although to be taken with caution,⁵⁹ suggest that in H46L/Q47L mesoGlbN* the final turn of the H helix becomes a mobile random coil. Unfolding the C-terminus of GlbN creates a necessary opening between His70 and His117. Overall, however, the helices of GlbN are largely maintained in GlbN*, which explains the relatively unchanged far-UV CD spectrum.

The interfaces formed between helices in H46L/Q47L mesoGlbN* were probed with a ¹³CH₃-edited NOESY experiment, portions of which are shown in Figure S8. Many of the observed long-range NOEs (Table S3) could be predicted from the crystal structure of WT GlbN bound to cyanide (PDB entry 1S69).¹⁴ NOEs among Leu4, Leu8, Phe55, Leu104, and Val108 define the interfaces of the A, E, and G helices.

Hydrophobic residues on the B, E, and G helices form the core of GlbN, and an extensive network involving Phe21, Tyr22, Val25, Leu47, Val87, and Leu91 indicates a conserved arrangement of these helices in the distal variant. Dipolar contacts between Leu92 and Ala109 (not shown) are consistent with the interface between the G helix and the N-terminal portion of the H helix.

In a flagrant departure from the WT structure, NOEs are observed between the E and F helices, arising from Gln43, Leu47, Phe50, Ala69, His70, and Leu73 (Figure 9). These helices are on opposite faces of the heme in all globins but are brought into the proximity of each other in H46L/Q47L mesoGlbN*. These new contacts provide strong evidence of the displacement of the heme group. Also of note is the environment of Tyr22 (B10). This residue is in the proximity of Phe21, faces inward toward the canonical distal heme pocket, and has an α -NH proton in slow exchange with the solvent (chemical shift time scale). NOEs to Val18, Val25, Leu47, and Leu73 describe a hydrophobic site likely responsible for the protection of the hydroxyl group (Figure S9). At the beginning of the G helix, the upfield shift of Asn80 NH in both ¹H and ¹⁵N and low protection factor determined by hydrogen–deuterium exchange (not shown) demonstrate perturbation of the conserved G helix N-cap.⁶⁰ This perturbation provides a convenient signature for GlbN*.

Repositioning the heme within GlbN is accompanied by the creation of an E–F interface and, as mentioned above, involves a separation of the F and H helices. Residues forming the binding site in H46L/Q47L mesoGlbN* were identified with NOEs between the polypeptide and the mesoheme. In WT GlbN, the B and C pyrroles are buried among hydrophobic residues in the core of the protein. Contacts between this portion of mesoheme and Phe50, Leu79, Phe84, and Val87 are observed in GlbN* and highlight common features of the two conformations. In contrast, the A and D pyrroles normally fit between the E and F helices to face the solvent, but in GlbN*, Leu122 is found in the proximity of the 5-CH₃ group. Also informative are contacts between Phe50 and His70 and between His117 and Phe84. A few key protein–mesoheme NOEs are shown in Figure S10 and listed in Table S2.

In summary, replacement of His46 in GlbN causes the heme to pivot about the pyrrole B/C half of the heme molecule and to slide between the F and H helices. The F helix packs against the E helix, filling the void created by heme displacement, while the C-terminus of the protein unfolds,

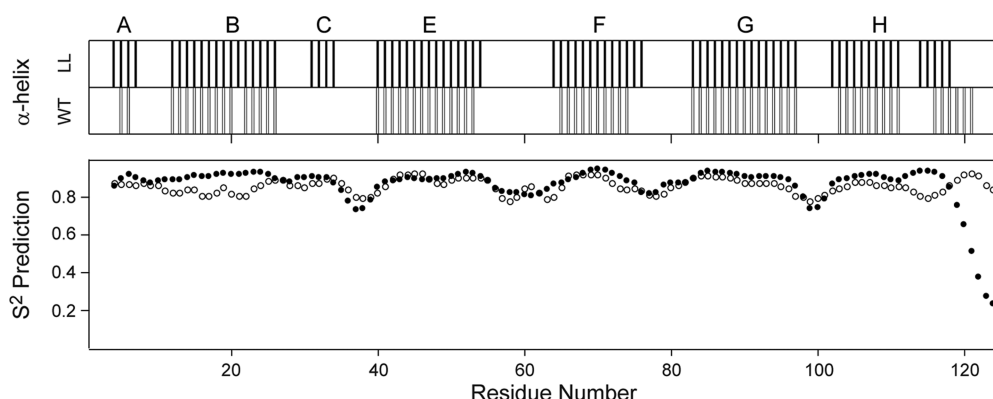


Figure 8. TALOS+ prediction of α -helical secondary structure (top, confidence level of >0.3) and ¹⁵N order parameters (bottom) using the H^N, H^a, C^a, C^b, N, and C' chemical shifts of H46L/Q47L mesoGlbN* ("LL", filled symbols) and WT GlbN (empty symbols, BMRB entry 5269). The letters above the figure denote the helices in WT GlbN.

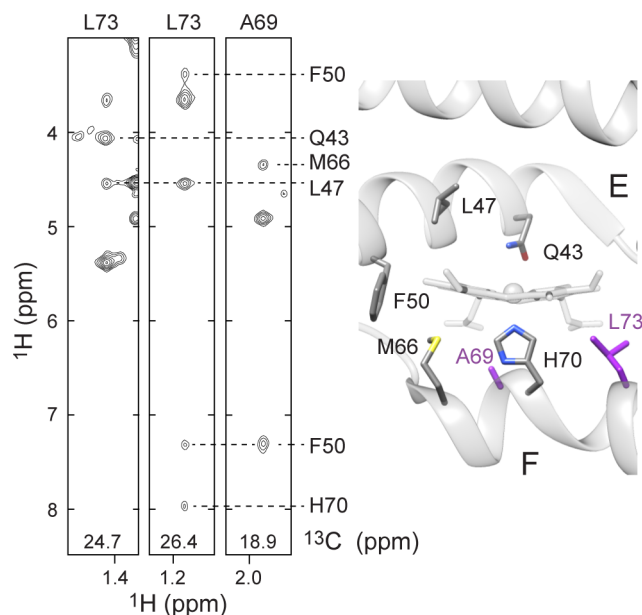


Figure 9. NOESY cross peaks observed for Leu73 and Ala69 in H46L/Q47L mesoGlbN. Portions of the $^{13}\text{CH}_3$ selective NOESY data displaying the CH_3 groups of Leu73 and Ala69 are shown on the left. Cross peaks to Phe50 H^{β} , Gln43 H^{α} , Met66 H^{α} , Leu47 H^{α} , Phe50 $\text{H}^{\beta 1/\beta 2}$, and His70 H^{α} are labeled. Unlabeled peaks correspond to intraresidue NOEs. The relevant residues are shown on the right using the crystal structure of cyanomet GlbN (PDB entry 1S69).¹⁴ Leu73 and Ala69 are colored purple. The Gln47Leu replacement was generated with Chimera.⁶¹ In this structure, the distance between Leu73 and Leu47 is >15 Å. The observed NOEs require the relative repositioning of the E and F helices and the removal of the intervening heme.

opening the needed gap between His70 and His117. The heme propionates remain exposed to the solvent. The overall globin fold and the core formed by hydrophobic residues in the B, E, and G helices are maintained in the new structure, schematized in Figure 10.

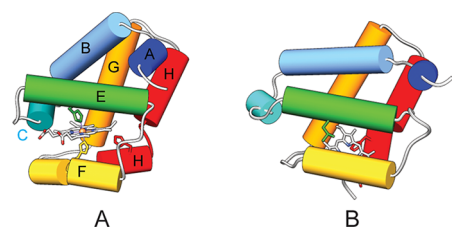


Figure 10. Structural representations of GlbN. (A) Bis-histidine GlbN (PDB entry 1RTX). (B) Model of GlbN* accounting for TALOS+ secondary structure and NOEs detected in H46L/Q47L mesoGlbN*. Note the changed position of the heme group.

Release of Heme from Ferric H46L GlbN*. A change in heme binding site is expected to affect heme affinity. Monitoring the transfer of ferric *b* heme from GlbN to apoMb is a convenient means of determining the rate of dissociation of the heme from the holoprotein.⁶² Addition of excess apoMb to a sample of H46L GlbN* resulted in conversion of the optical spectrum to that of aquomet Mb (Figure 11). Singular-value decomposition of the spectra and global analysis display mono-phasic kinetics with an apparent rate constant of $(3.1 \pm 0.1) \times 10^{-3} \text{ s}^{-1}$. The mechanistic details (e.g., relation to rotational

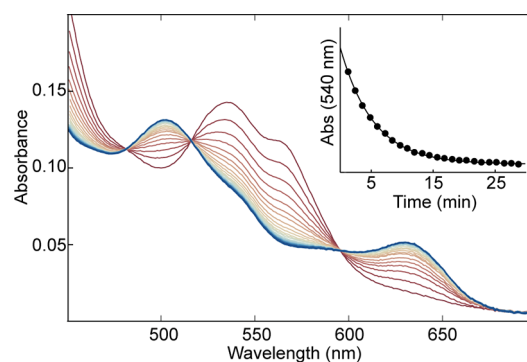


Figure 11. Transfer of ferric *b* heme from H46L GlbN ($10 \mu\text{M}$) to apoMb ($100 \mu\text{M}$) at pH 7.2. The spectrum of H46L GlbN (red) is converted to the spectrum of aquomet Mb (blue). The inset shows the decrease in absorbance at 540 nm in time and the best fit to a single-exponential decay.

isomer population) are unclear, but the observed rate is ~ 1000 -fold faster than that observed for the major kinetic phase of WT GlbN under similar conditions.⁴ Assuming that the association rate constant, k_{on} , is unchanged,⁶³ the increased off rate represents a lower heme affinity in the variant. Consistent with a loss of binding energy and stability, a decrease in the T_m of ~ 10 °C was previously reported for H46L GlbN,¹⁶ and increasing the hydrostatic pressure causes a loss of heme resonances and spectral resolution relatively early⁶⁴ in the pressure titration (Figure S11).

Heme Cross-Linking in Ferrous GlbN Variants. GlbN is remarkable for forming a covalent linkage between the heme and His117²⁴ (Figure S12A). Recombinant GlbN is prepared in the ferric state, and addition of a reducing agent, typically DT, causes complete formation of the bond on the millisecond time scale at neutral pH.⁶⁵ H46L GlbN* undergoes the same post-translational modification (PTM) but is less reactive.¹⁶ Prolonged incubation of H46L/Q47L GlbN* with DT followed by reoxidation and removal of DT byproducts revealed partial formation of the heme–protein adduct, which displays high-spin features consistent with the loss of His117 iron coordination (Figure S12B). Cross-linking requires the heme to adopt the correct orientation with respect to His117, the sliding of the heme back to its canonical site perhaps contributing to the decreased reaction rate in the H46 variants.

The ability of His117 to both coordinate the ferrous iron and undergo irreversible covalent modification was explored with heme transfer experiments and by making use of mesoGlbN. Because vinyl groups are absent from mesoheme, mesoGlbN complexes provide access to the ferrous state without PTM. The optical spectrum of ferrous H46L/Q47L mesoGlbN displays two resolved Soret peaks, one presumably corresponding to a high-spin form with a maximum at $\sim 426 \text{ nm}$ and the other to a low-spin form with a maximum at $\sim 415 \text{ nm}$ (Figure 12A). The mixture represents partial His117 coordination, and the appearance of the NMR spectrum (not shown) demonstrates that interconversion between low- and high-spin species occurs rapidly on the chemical shift time scale. The coexistence of GlbN* and GlbN illustrates that bis-histidine coordination in GlbN* is weaker in the ferrous state than in the ferric state.^{66,67}

To inspect the kinetics of PTM formation, H46L GlbN containing a *b* heme was placed in the presence of apoMb and immediately reduced by DT (Figure 12B). In the absence of apoMb, freshly reduced H46L GlbN shows spectral changes over the course of hours (not shown). When excess apoMb is

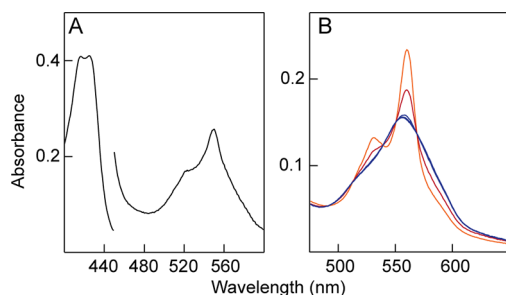


Figure 12. (A) Optical spectrum of ferrous H46L/Q47L mesoGlbN at neutral pH. The visible region of the spectrum has been amplified 5-fold. (B) Transfer of ferrous *b* heme from H46L GlbN to apoMb. The spectrum of ferrous H46L GlbN immediately following reduction is colored orange. Upon addition of a reducing agent and apoMb, a fraction of ferrous H46L GlbN is observed (red trace, ~10 s after mixing) before complete conversion to deoxy Mb (blue traces). The orange spectrum was scaled according to the isosbestic point at 559 nm for ease of comparison.

available, nearly complete loss of the ferrous heme occurred during the dead time of the manual mixing experiment. For comparison, reduced H117A GlbN releases heme with a half-life of ~1 h,⁶⁷ and WT GlbN forms the PTM immediately.¹⁶ Thus, ferrous H46L GlbN is a dynamic species that exhibits transient His117 ligation (GlbN*), gradual PTM formation, and rapid dissociation of the heme group.

■ DISCUSSION

Factors Allowing His117 Coordination in H46L GlbN.

Positioning the heme between the F and H helices requires conformational adjustments to the WT structure (Figure 9). The disordered EF loop undergoes a large structural change when WT GlbN binds an exogenous ligand (Figure 1),¹⁴ the same flexible loop allows the F helix to form a new interface in mesoGlbN*. In the H helix beyond Ala112, rapid backbone NH/ND exchange⁵⁵ indicates a propensity for structure opening. This region also participates in the rearrangement. Although the intrinsic plasticity of the EF loop and low conformational stability at the end of the H helix were known features of GlbN expected to facilitate a low-energy deformation of the structure, the perturbation of a conserved helix-capping H-bond at the beginning of the G helix⁶⁰ was not. Formation of the Fe–His117 coordination bond apparently offsets the cumulative losses of conformational stability associated with the distortion of the canonical holoprotein structure.

Further insight can be derived with cyanide binding to GlbN*. As observed in prior work, the NMR spectrum of cyanomet H46L GlbN resembles closely that of WT GlbN,¹⁶ including evidence of Tyr22–cyanide interaction. This implies that cyanide displaces His117 from the iron and restores the native (cyanomet) GlbN structure. In support of this interpretation, binding of cyanide, imidazole, or azide to H46L/Q47L GlbN restores the helix-capping H-bond between Asn80 and His83 (Figure S13A). Subsequent removal of imidazole or azide by extensive buffer exchange yields the starting GlbN* complex (Figure S13B), demonstrating reversible movement of the heme within the protein matrix. A plausible interpretation is that simultaneous coordination of His117 and His70 propagates strains from each Fe–N ε 2 linkage (or N δ 1 linkage, a possibility that is not eliminated by the available data) to the backbone, strains that are compensated by ligation. Once an exogenous ligand binds, the H helix is released, strains on the

proximal side are relieved, and the heme migrates to the WT, energetically more favorable site lined with hydrophobic residues and consolidated by the hydrogen bond network composed of Tyr22, Gln43, and Gln47.

A related GlbN from the cyanobacterium *Synechococcus* PCC sp. 7002 provides additional information about the determinants of His117 ligation. *Synechococcus* GlbN also coordinates the heme iron with His70 and His46 and is capable of the same heme–His117 PTM.⁶⁸ The H46L variant of *Synechococcus* GlbN, however, forms an aquomet complex in the ferric state with the heme presumably in its normal site.⁶⁵ Although it is not possible to infer binding energies from structure, striking differences in the H helices of the two proteins are likely relevant to the relative affinities of the alternative binding site. In *Synechocystis* GlbN, the sequence directly upstream of His117 is rich in alanines (¹⁰⁹AAVAGAPA, Gly113 underlined), whereas in *Synechococcus* GlbN, it is proline-less and has several β -branched residues, (¹⁰⁹VTIVGSVQ). On the basis of the sequence alone, the helical propensity in this region is higher in *Synechocystis* GlbN than in *Synechococcus* GlbN, which may contribute to a favorable orientation of His117 for coordination.

A survey of sequences related to GlbN mapped onto known three-dimensional structures reveal that most proteins have a two-residue deletion at positions 114 and 115. The sequences containing a histidine at GlbN's positions 117 do not have this deletion and fall roughly in two categories; either the 109–116 segment is Ala-rich or not. Furthermore, His117 is systematically found in combination with His46, except in *Microcystis aeruginosa* HbN (WP_004161553), which harbors the Tyr46/His117 pair and the ¹⁰⁹VQIVGSVT sequence. In GlbN*, the mesoheme contacts Ala112. Val112, in *Synechococcus* GlbN and presumably other proteins containing this residue, forms a hydrophobic core with the conserved Phe50 (E14) and Phe84 (G5) along with Val109 and Ile111.⁶⁹ Compared to those afforded by Ala112, these interactions may be sufficient to counteract the energetic benefit of His117 ligation. Hypotheses such as these can be tested with a combination of mutagenesis and NMR characterization to refine the understanding of heme site preference.

Relation to Apoprotein Properties. The thermodynamic view presented above draws attention to the apoprotein as an agent guiding the preference for GlbN or GlbN*. It is reasonable to assume that an initial state endowed with preexisting, stable, and distinctive holoGlbN features would be less likely to populate the holoGlbN* conformation. Conversely, an unstable apoprotein may be more permissive. In *Synechococcus* apoGlbN, portions of the B, G, and H helices form a core that unfolds cooperatively upon heating.⁷⁰ The ¹H–¹⁵N HSQC spectrum is resolved, and chemical shifts suggest that the N-terminal portion of the H helix is folded. In contrast, *Synechocystis* apoGlbN, which has a much reduced helical content compared to that of the holoprotein⁴ and no native baseline in urea denaturation experiments,⁷¹ has a poorly resolved ¹⁵N–¹H HSQC spectrum, a property shared by H46L/Q47L apoGlbN (Figure S14).

The apoprotein stability and folding mechanism have not yet been extensively explored in the 2-on-2 globin lineage. To condition expectations, it is useful to draw a parallel to 3-on-3 globins. In sperm whale apomyoglobin, the A, B, and E helices and parts of the G and H helices pack to form a hydrophobic core whereas the E/F loop, F helix, F/G turn, and C-terminal end of the H helix are dynamic elements.^{72–75}

In general, 3-on-3 apoglobins display a variety of folding pathways and intermediate population to reach their native state.^{76–79} The stability of this state is known to depend on the amino acid makeup of the core and heme binding site.^{80–82} However, even highly destabilized 3-on-3 apoproteins can refold into the expected holoprotein structure upon heme binding.⁸⁰ The truncated A helix and shorter H helix of the group 1 2-on-2 fold eliminate several of the interactions that are observed in the 3-on-3 proteins. Among 2-on-2 globins, the extent of the hydrophobic core, e.g., the participation of Val109 and Val112 in *Synechococcus* GlbN, varies and likely contributes to both the structural stability of the apoprotein and the accessibility of alternative holoprotein conformations. Globins that have a low level of apoprotein structure, such as *Synechocystis* GlbN, may have a stronger propensity for non-canonical heme binding, although this initial state property is clearly not a sufficient condition. Additional data factoring in final state characteristics are needed to probe such a connection.

Distal Ligation Competition. Dioxygen binding is a defining feature of globins, whether for transport, storage, or chemistry. Competition between endogenous and exogenous coordination is a well-known property of most “hexacoordinate” hemoglobins.⁸ The persistence of a non-native bis-histidine structure upon the replacement of a single amino acid in GlbN highlights the facility with which a heme group can associate with nitrogenous ligands and lead to internal competition for the iron. His/Lys ligand switching, for example, can be driven by altering solution conditions, most notably pH as shown in cytochrome *c*^{83,84} and *Synechococcus* GlbN.⁸⁵ Internal ligand exchange is observed in other guises, as well, illustrated in the signaling mechanism of CooA⁸⁶ and the heme transfer mechanism of PhuS.^{87,88} Nonspecific or transient binding is also a hallmark of heme–protein interactions.^{63,89,90} Most often, the architecture and flexibility of the protein create a unique heme binding site with a constant set of ligands. In a sense, *Synechococcus* and *Synechocystis* GlbNs illustrate a gradation in the strength of “nonspecific” binding, with *Synechocystis* H46L GlbN being an extreme example of competition and stabilization.

Reconciliation of H46 Variant Observations. In light of alternative ligation, the role of the interfering His117 should be scrutinized anew. Covalent attachment of the heme to His117 by addition to a vinyl is observed in *Synechococcus* cells⁹¹ and presumably other cyanobacterial HbNs. The PTM offers the advantage of heme retention, which may be important under some cellular conditions. We have proposed that His46 drives the heme to the correct site for PTM.¹⁰ We now show that free His117 has a strong tendency to coordinate the heme iron and reinforce our structural explanation for the requirement of His46. PTM and rogue ligation may also explain the rare occurrence of a histidine at topological position 117. One possible role for His117 besides PTM is to assist apoGlbN in the acquisition of free heme. To return to an extensively studied system, folding of apoMb occurs through a three-state mechanism, and the unfolded, intermediate, and native states display progressively increasing heme affinities.¹⁰ Partially folded apoMb incorporates heme to give a bis-histidine hemichrome that readily converts to the structured holoprotein, illustrating how metal ions and coordination chemistry can shape protein folding pathways. On-pathway intermediates must undergo ligand exchange to produce the folded protein efficiently. The fact that transient His117 coordination is observed in ferrous H46L GlbN may speak to this point.

Gradual formation of the covalent heme modification in this protein demonstrates that the bis-histidine GlbN* complex is capable of converting to GlbN. His117, attached to a terminal and flexible part of the protein, could offer a means of recruiting free ferrous heme to apoGlbN by coordinating the iron opposite His70, rapidly exchanging with His46 to generate the native state, and securing the cofactor with a covalent linkage.

The unusual structure of GlbN* clarifies other observations made on H46 variants. A greater degree of high-spin character in ferric H46A GlbN,^{7,16} as compared to ferric H46L GlbN, can be ascribed to a competition between native GlbN and GlbN* conformations in the variants. Leu46 contributes to the hydrophobic core of GlbN*, while Ala46 could promote the GlbN structure by facilitating the coordination of a solvent molecule to the distal iron site. CO binding kinetics have been measured for H46A GlbN.⁵ Discrepancies between results from rapid mixing and flash photolysis experiments can be explained by movement of the cofactor within the polypeptide. A slow phase ($\sim 0.01\text{ s}^{-1}$, independent of CO concentration) observed by rapid mixing may reflect migration of the cofactor back to the standard heme pocket.

Perspective on Globin Mutagenesis and Homology

Modeling. Beyond the novelty of the GlbN* structure, our results offer some generic perspective on heme binding. They emphasize that a single-amino acid replacement in the heme cavity can have hard-to-detect but profound consequences. It is customary to replace a suspected heme axial ligand to confirm a coordination scheme or pursue thermodynamic and kinetic studies of hexacoordination, but as shown here, data collected with such variants may reflect perturbations much larger than breaking a bond and allowing solvent in the heme pocket. The complexity of heme protein analysis is well illustrated with GlbN, which displays heme orientational disorder, PTM, and uniquely behaved distal variants. GlbN* also highlights the potential for distortion of a holoprotein without extraordinary global reshaping. The results call into question the validity of simple homology modeling or a computational approach resting solely on wild-type structural assumptions.

ASSOCIATED CONTENT

Supporting Information

The Supporting Information is available free of charge on the ACS Publications website at DOI: [10.1021/acs.biochem.8b00752](https://doi.org/10.1021/acs.biochem.8b00752).

Tables of chemical shifts, longitudinal relaxation times, and nuclear Overhauser effects; NMR spectra for longitudinal relaxation time determination and intensity recovery plots; assigned ^1H – ^{15}N HSQC spectra; portions of NOESY spectra, chemical shift perturbation plots, NOE diagrams, and ^1H – ^{15}N HSQC spectra supporting the reversible relocation of the heme and minor secondary structure alterations; apoprotein ^1H – ^{15}N HSQC spectra and pressure response of NMR data; and electronic absorption spectra and their response to pH (PDF)

AUTHOR INFORMATION

Corresponding Author

*E-mail: lecomte_jtj@jhu.edu. Telephone: (410) 516-7019.

ORCID

Juliette T. J. Lecomte: 0000-0003-1116-0053

Funding

This work was supported by the National Science Foundation Grant MCB-1330488 to J.T.J.L. and National Institutes of Health Grant T32 GM080189 (D.B.N.).

Notes

The authors declare no competing financial interest.

ACKNOWLEDGMENTS

The authors thank Dr. Katherine Tripp for help with CD data collection, Dr. Ananya Majumdar of the JHU Biomolecular NMR Center for help with NMR data collection, Dr. Matthew Preimesberger for helpful discussions, Dr. Christopher Falzone for careful reading of the manuscript, and Christos Kougantakis for preliminary experiments and assistance with non-uniformly sampled NMR data.

ABBREVIATIONS

1D, one-dimensional; 2D, two-dimensional; 3D, three-dimensional; apoMb, horse skeletal muscle apomyoglobin; CD, circular dichroism; DT, sodium dithionite; GlbN, *Synechocystis* sp. PCC 6803 hemoglobin; GlbN-A, GlbN with covalently attached heme; GlbN*, GlbN with His70 and His117 as heme axial ligands; heme *b*, Fe-protoporphyrin IX; HSQC, heteronuclear single-quantum coherence; Mb, myoglobin; mesoGlbN, GlbN reconstituted with mesoheme; mesoheme, Fe-mesoporphyrin IX; met, ferric; NOE, nuclear Overhauser effect; PDB, Protein Data Bank; pH*, pH uncorrected for isotope effect; PTM, post-translational modification; rmsd, root-mean-square deviation; *T*₁, spin-lattice (longitudinal) relaxation time; WT, wild-type.

REFERENCES

- Wajcman, H., Kiger, L., and Marden, M. C. (2009) Structure and function evolution in the superfamily of globins. *C. R. Biol.* 332, 273–282.
- Vinogradov, S. N., Tinajero-Trejo, M., Poole, R. K., and Hoogewijs, D. (2013) Bacterial and archaeal globins — A revised perspective. *Biochim. Biophys. Acta, Proteins Proteomics* 1834, 1789–1800.
- Gardner, P. R. (2012) Hemoglobin: A nitric-oxide dioxygenase. *Scientifica* 2012, 34.
- Lecomte, J. T. J., Scott, N. L., Vu, B. C., and Falzone, C. J. (2001) Binding of ferric heme by the recombinant globin from the cyanobacterium *Synechocystis* sp. PCC 6803. *Biochemistry* 40, 6541–6552.
- Hvitved, A. N., Trent, J. T., 3rd, Premer, S. A., and Hargrove, M. S. (2001) Ligand binding and hexacoordination in *Synechocystis* hemoglobin. *J. Biol. Chem.* 276, 34714–34721.
- Das, T. K., Couture, M., Ouellet, Y., Guertin, M., and Rousseau, D. L. (2001) Simultaneous observation of the O–O and Fe–O₂ stretching modes in oxyhemoglobins. *Proc. Natl. Acad. Sci. U. S. A.* 98, 479–484.
- Couture, M., Das, T. K., Savard, P. Y., Ouellet, Y., Wittenberg, J. B., Wittenberg, B. A., Rousseau, D. L., and Guertin, M. (2000) Structural investigations of the hemoglobin of the cyanobacterium *Synechocystis* PCC 6803 reveal a unique distal heme pocket. *Eur. J. Biochem.* 267, 4770–4780.
- Kakar, S., Hoffman, F. G., Storz, J. F., Fabian, M., and Hargrove, M. S. (2010) Structure and reactivity of hexacoordinate hemoglobins. *Biophys. Chem.* 152, 1–14.
- Rifkind, J. M., Abugo, O., Levy, A., and Heim, J. (1994) Detection, formation, and relevance of hemichromes and hemochromes. *Methods Enzymol.* 231, 449–480.
- Culbertson, D. S., and Olson, J. S. (2010) Role of heme in the unfolding and assembly of myoglobin. *Biochemistry* 49, 6052–6063.
- Mollan, T. L., Khandros, E., Weiss, M. J., and Olson, J. S. (2012) Kinetics of α -globin binding to α -hemoglobin stabilizing protein (AHSP) indicate preferential stabilization of hemichrome folding intermediate. *J. Biol. Chem.* 287, 11338–11350.
- Halder, P., Trent, J. T., 3rd, and Hargrove, M. S. (2007) Influence of the protein matrix on intramolecular histidine ligation in ferric and ferrous hexacoordinate hemoglobins. *Proteins: Struct., Funct., Genet.* 66, 172–182.
- Hoy, J. A., Kundu, S., Trent, J. T., 3rd, Ramaswamy, S., and Hargrove, M. S. (2004) The crystal structure of *Synechocystis* hemoglobin with a covalent heme linkage. *J. Biol. Chem.* 279, 16535–16542.
- Trent, J. T., 3rd, Kundu, S., Hoy, J. A., and Hargrove, M. S. (2004) Crystallographic analysis of *Synechocystis* cyanoglobin reveals the structural changes accompanying ligand binding in a hexacoordinate hemoglobin. *J. Mol. Biol.* 341, 1097–1108.
- Lecomte, J. T. J., Vu, B. C., and Falzone, C. J. (2005) Structural and dynamic properties of *Synechocystis* sp. PCC 6803 Hb revealed by reconstitution with Zn-protoporphyrin IX. *J. Inorg. Biochem.* 99, 1585–1592.
- Nothnagel, H. J., Love, N., and Lecomte, J. T. J. (2009) The role of the heme distal ligand in the post-translational modification of *Synechocystis* hemoglobin. *J. Inorg. Biochem.* 103, 107–116.
- Scott, N. L., and Lecomte, J. T. J. (2000) Cloning, expression, purification, and preliminary characterization of a putative hemoglobin from the cyanobacterium *Synechocystis* sp. PCC 6803. *Protein Sci.* 9, 587–597.
- Teale, F. W. J. (1959) Cleavage of heme-protein link by acid methylethylketone. *Biochim. Biophys. Acta* 35, 543.
- Johnson, E. A., Rice, S. L., Preimesberger, M. R., Nye, D. B., Gilevicius, L., Wenke, B. B., Brown, J. M., Witman, G. B., and Lecomte, J. T. J. (2014) Characterization of THB1, a *Chlamydomonas reinhardtii* truncated hemoglobin: linkage to nitrogen metabolism and identification of lysine as the distal heme ligand. *Biochemistry* 53, 4573–4589.
- de Duve, C., Ågren, G., and Gjertsen, P. (1948) A spectrophotometric method for the simultaneous determination of myoglobin and hemoglobin in extracts of human muscle. *Acta Chem. Scand.* 2, 264–289.
- Antonini, E., Brunori, M., Caputo, A., Chiancone, E., Fanelli, A. R., and Wyman, J. (1964) Studies on the structure of hemoglobin: III. Physicochemical properties of reconstituted hemoglobins. *Biochim. Biophys. Acta, Spec. Sect. Biophys. Subj.* 79, 284–292.
- Gill, S. C., and von Hippel, P. H. (1989) Calculation of protein extinction coefficients from amino acid sequence data. *Anal. Biochem.* 182, 319–326.
- Hargrove, M. S., Singleton, E. W., Quillin, M. L., Ortiz, L. A., Phillips, G. N., Jr., Olson, J. S., and Mathews, A. J. (1994) His64(E7)–>Tyr apomyoglobin as a reagent for measuring rates of hemin dissociation. *J. Biol. Chem.* 269, 4207–4214.
- Vu, B. C., Jones, A. D., and Lecomte, J. T. J. (2002) Novel histidine-heme covalent linkage in a hemoglobin. *J. Am. Chem. Soc.* 124, 8544–8545.
- Preimesberger, M. R., Pond, M. P., Majumdar, A., and Lecomte, J. T. J. (2012) Electron self-exchange and self-amplified posttranslational modification in the hemoglobins from *Synechocystis* sp. PCC 6803 and *Synechococcus* sp. PCC 7002. *JBIC, J. Biol. Inorg. Chem.* 17, 599–609.
- Wishart, D. S., Bigam, C. G., Yao, J., Abildgaard, F., Dyson, H. J., Oldfield, E., Markley, J. L., and Sykes, B. D. (1995) ¹H, ¹³C and ¹⁵N chemical shift referencing in biomolecular NMR. *J. Biomol. NMR* 6, 135–140.
- Delaglio, F., Grzesiek, S., Vuister, G. W., Zhu, G., Pfeifer, J., and Bax, A. (1995) NMRPipe: a multidimensional spectral processing system based on UNIX pipes. *J. Biomol. NMR* 6, 277–293.
- Goddard, T. D., and Kneller, D. G. (2006) SPARKY 3, University of California, San Francisco.
- Hyberts, S. G., Takeuchi, K., and Wagner, G. (2010) Poisson-gap sampling and forward maximum entropy reconstruction for

enhancing the resolution and sensitivity of protein NMR data. *J. Am. Chem. Soc.* 132, 2145–2147.

(30) Sun, S., Gill, M., Li, Y., Huang, M., and Byrd, R. A. (2015) Efficient and generalized processing of multidimensional NUS NMR data: the NESTA algorithm and comparison of regularization terms. *J. Biomol. NMR* 62, 105–117.

(31) Maciejewski, M. W., Schuyler, A. D., Gryk, M. R., Moraru, II, Romero, P. R., Ulrich, E. L., Eghbalnia, H. R., Livny, M., Delaglio, F., and Hoch, J. C. (2017) NMRbox: A resource for biomolecular NMR computation. *Biophys. J.* 112, 1529–1534.

(32) Marion, D., Driscoll, P. C., Kay, L. E., Wingfield, P. T., Bax, A., Gronenborn, A. M., and Clore, G. M. (1989) Overcoming the overlap problem in the assignment of ^1H NMR spectra of larger proteins by use of three-dimensional heteronuclear ^1H - ^{15}N Hartmann-Hahn-multiple quantum coherence and nuclear Overhauser-multiple quantum coherence spectroscopy: application to interleukin 1 β . *Biochemistry* 28, 6150–6156.

(33) Kay, L. E., Ikura, M., Tschudin, R., and Bax, A. (1990) Three-dimensional triple-resonance NMR spectroscopy of isotopically enriched proteins. *J. Magn. Reson.* 89, 496–514.

(34) Grzesiek, S., and Bax, A. (1992) Correlating backbone amide and side chain resonances in larger proteins by multiple relayed triple resonance NMR. *J. Am. Chem. Soc.* 114, 6291–6293.

(35) Wittekind, M., and Mueller, L. (1993) HNCACB, a high-sensitivity 3D NMR experiment to correlate amide-proton and nitrogen resonances with the alpha- and beta-carbon resonances in proteins. *J. Magn. Reson., Ser. B* 101, 201–205.

(36) Montelione, G. T., Lyons, B. A., Emerson, S. D., and Tashiro, M. (1992) An efficient triple resonance experiment using carbon-13 isotropic mixing for determining sequence-specific resonance assignments of isotopically-enriched proteins. *J. Am. Chem. Soc.* 114, 10974–10975.

(37) Bax, A., and Grzesiek, S. (1993) Methodological Advances in Protein NMR. In *NMR of Proteins* (Clore, G. M., and Gronenborn, A. M., Eds.) pp 33–52, Macmillan Education UK, London.

(38) La Mar, G. N., Satterlee, J. D., and de Ropp, J. S. (2000) Nuclear magnetic resonance of hemoproteins. In *The Porphyrin Handbook* (Smith, K. M., Kadish, K., and Guillard, R., Eds.) pp 185–298, Academic Press, Burlington, MA.

(39) Antonini, E., and Brunori, M. (1971) *Hemoglobin and myoglobin in their reactions with ligands*, Vol. 12, North-Holland, Amsterdam.

(40) Nagao, S., Hirai, Y., Suzuki, A., and Yamamoto, Y. (2005) ^{19}F NMR characterization of the thermodynamics and dynamics of the acid–alkaline transition in a reconstituted sperm whale metmyoglobin. *J. Am. Chem. Soc.* 127, 4146–4147.

(41) Bren, K. L., and Gray, H. B. (1993) Structurally engineered cytochromes with novel ligand-binding sites: oxy and carbon monoxo derivatives of semisynthetic horse heart Ala80 cytochrome c. *J. Am. Chem. Soc.* 115, 10382–10383.

(42) Banci, L., Bertini, I., Bren, K. L., Gray, H. B., and Turano, P. (1995) pH-dependent equilibria of yeast Met80Ala-iso-1-cytochrome c probed by NMR spectroscopy: a comparison with the wild-type protein. *Chem. Biol.* 2, 377–383.

(43) McGrath, T. M., and La Mar, G. N. (1978) Proton NMR study of the thermodynamics and kinetics of the acid in equilibrium base transitions in reconstituted metmyoglobins. *Biochim. Biophys. Acta, Protein Struct.* 534, 99–111.

(44) Shibata, T., Nagao, S., Fukaya, M., Tai, H., Nagatomo, S., Morihashi, K., Matsuo, T., Hirota, S., Suzuki, A., Imai, K., and Yamamoto, Y. (2010) Effect of heme modification on oxygen affinity of myoglobin and equilibrium of the acid-alkaline transition in metmyoglobin. *J. Am. Chem. Soc.* 132, 6091–6098.

(45) Qin, J., La Mar, G. N., Dou, Y., Admiraal, S. J., and Ikeda-Saito, M. (1994) ^1H NMR study of the solution molecular and electronic structure of engineered distal myoglobin His64(E7) Val/Val68(E11) His double mutant. Coordination of His64(E11) at the sixth position in both low-spin and high-spin states. *J. Biol. Chem.* 269, 1083–1090.

(46) La Mar, G. N., Viscio, D. B., Smith, K. M., Caughey, W. S., and Smith, M. L. (1978) NMR studies of low-spin ferric complexes of natural porphyrin derivatives. 1. Effect of peripheral substituents on the π electronic asymmetry in biscyano complexes. *J. Am. Chem. Soc.* 100, 8085–8092.

(47) Hirai, Y., Yamamoto, Y., and Suzuki, A. (2000) ^{19}F NMR study of the heme orientation and electronic structure in a myoglobin reconstituted with a ring-fluorinated heme. *Bull. Chem. Soc. Jpn.* 73, 2309–2316.

(48) Bertini, I., Luchinat, C., Parigi, G., and Walker, F. A. (1999) Heme methyl ^1H chemical shifts as structural parameters in some low-spin ferriheme proteins. *JBIC, J. Biol. Inorg. Chem.* 4, 515–519.

(49) La Mar, G. N., and Walker, F. A., Eds. (1979) *Nuclear magnetic resonance of paramagnetic metalloporphyrins*, Vol. 4, Academic Press, New York.

(50) Unger, S. W., Jue, T., and La Mar, G. N. (1985) Proton NMR dipolar relaxation by delocalized spin density in low-spin ferric porphyrin complexes. *J. Magn. Reson.* 61, 448–456.

(51) Mortuza, G. B., and Whitford, D. (1997) Mutagenesis of residues 27 and 78 modulates heme orientation in cytochrome b_5 . *FEBS Lett.* 412, 610–614.

(52) Cocco, M. J., Barrick, D., Taylor, S. V., and Lecomte, J. T. J. (1992) Histidine 82 influences heme orientational isomerism in sperm whale myoglobin. Long-range effect due to mutation of a conserved residue. *J. Am. Chem. Soc.* 114, 11000–11001.

(53) Yang, F., Zhang, H., and Knipp, M. (2009) A one-residue switch reverses the orientation of a heme b cofactor. Investigations of the ferriheme NO transporters nitrophorin 2 and 7 from the blood-feeding insect *Rhodnius prolixus*. *Biochemistry* 48, 235–241.

(54) Sarma, S., DiGate, R. J., Banville, D. L., and Guiles, R. D. (1996) ^1H , ^{13}C and ^{15}N NMR assignments and secondary structure of the paramagnetic form of rat cytochrome b_5 . *J. Biomol. NMR* 8, 171–183.

(55) Falzone, C. J., Vu, B. C., Scott, N. L., and Lecomte, J. T. J. (2002) The solution structure of the recombinant hemoglobin from the cyanobacterium *Synechocystis* sp. PCC 6803 in its hemichrome state. *J. Mol. Biol.* 324, 1015–1029.

(56) Nagai, M., Kobayashi, C., Nagai, Y., Imai, K., Mizusawa, N., Sakurai, H., Neya, S., Kayanuma, M., Shoji, M., and Nagatomo, S. (2015) Involvement of propionate side chains of the heme in circular dichroism of myoglobin: experimental and theoretical analyses. *J. Phys. Chem. B* 119, 1275–1287.

(57) Shen, Y., Delaglio, F., Cornilescu, G., and Bax, A. (2009) TALOS+: A hybrid method for predicting protein backbone torsion angles from NMR chemical shifts. *J. Biomol. NMR* 44, 213–223.

(58) Falzone, C. J., and Lecomte, J. T. J. (2002) Assignment of the ^1H , ^{13}C , and ^{15}N signals of *Synechocystis* sp. PCC 6803 methemoglobin. *J. Biomol. NMR* 23, 71–72.

(59) Berjanskii, M. V., and Wishart, D. S. (2005) A simple method to predict protein flexibility using secondary chemical shifts. *J. Am. Chem. Soc.* 127, 14970–14971.

(60) Preimesberger, M. R., Majumdar, A., Rice, S. L., Que, L., and Lecomte, J. T. J. (2015) Helix-capping histidines: Diversity of N-H···N hydrogen bond strength revealed by $^{2\text{h}}\text{J}_{\text{NN}}$ scalar couplings. *Biochemistry* 54, 6896–6908.

(61) Pettersen, E. F., Goddard, T. D., Huang, C. C., Couch, G. S., Greenblatt, D. M., Meng, E. C., and Ferrin, T. E. (2004) UCSF Chimera - a visualization system for exploratory research and analysis. *J. Comput. Chem.* 25, 1605–1612.

(62) Hargrove, M. S., and Olson, J. S. (1996) The stability of holomyoglobin is determined by heme affinity. *Biochemistry* 35, 11310–11318.

(63) Hargrove, M. S., Barrick, D., and Olson, J. S. (1996) The association rate constant for heme binding to globin is independent of protein structure. *Biochemistry* 35, 11293–11299.

(64) Dellarole, M., Roumestand, C., Royer, C., and Lecomte, J. T. J. (2013) Volumetric properties underlying ligand binding in a monomeric hemoglobin: A high-pressure NMR study. *Biochim. Biophys. Acta, Proteins Proteomics* 1834, 1910–1922.

(65) Nothnagel, H. J., Preimesberger, M. R., Pond, M. P., Winer, B. Y., Adney, E. M., and Lecomte, J. T. J. (2011) Chemical reactivity of

Synechococcus sp. PCC 7002 and *Synechocystis* sp. PCC 6803 hemoglobins: covalent heme attachment and bishistidine coordination. *JBIC, J. Biol. Inorg. Chem.* 16, 539–552.

(66) Cowley, A. B., Kennedy, M. L., Silchenko, S., Lukat-Rodgers, G. S., Rodgers, K. R., and Benson, D. R. (2006) Insight into heme protein redox potential control and functional aspects of six-coordinate ligand-sensing heme proteins from studies of synthetic heme peptides. *Inorg. Chem.* 45, 9985–10001.

(67) Hoy, J. A., Smagghe, B. J., Halder, P., and Hargrove, M. S. (2007) Covalent heme attachment in *Synechocystis* hemoglobin is required to prevent ferrous heme dissociation. *Protein Sci.* 16, 250–260.

(68) Scott, N. L., Falzone, C. J., Vuletich, D. A., Zhao, J., Bryant, D. A., and Lecomte, J. T. J. (2002) The hemoglobin of the cyanobacterium *Synechococcus* sp. PCC 7002: Evidence for hexacoordination and covalent adduct formation in the ferric recombinant protein. *Biochemistry* 41, 6902–6910.

(69) Wenke, B. B., Lecomte, J. T. J., Héroux, A., and Schlessman, J. L. (2014) The 2/2 hemoglobin from the cyanobacterium *Synechococcus* sp. PCC 7002 with covalently attached heme: comparison of X-ray and NMR structures. *Proteins: Struct., Funct., Genet.* 82, 528–534.

(70) Vuletich, D. A., Falzone, C. J., and Lecomte, J. T. J. (2006) Structural and dynamic repercussions of heme binding and heme-protein cross-linking in *Synechococcus* sp. PCC 7002 hemoglobin. *Biochemistry* 45, 14075–14084.

(71) Knappenberger, J. A., Kuriakose, S. A., Vu, B. C., Nothnagel, H. J., Vuletich, D. A., and Lecomte, J. T. J. (2006) Proximal influences in two-on-two globins: Effect of the Ala69Ser replacement on *Synechocystis* sp. PCC 6803 hemoglobin. *Biochemistry* 45, 11401–11413.

(72) Cocco, M. J., and Lecomte, J. T. J. (1990) Characterization of hydrophobic cores in apomyoglobin: a proton NMR spectroscopy study. *Biochemistry* 29, 11067–11072.

(73) Hughson, F. M., Wright, P. E., and Baldwin, R. L. (1990) Structural characterization of a partly folded apomyoglobin intermediate. *Science* 249, 1544–1548.

(74) Lecomte, J. T. J., Sukits, S. F., Bhattacharya, S., and Falzone, C. J. (1999) Conformational properties of native sperm whale apomyoglobin in solution. *Protein Sci.* 8, 1484–1491.

(75) Landfried, D. A., Vuletich, D. A., Pond, M. P., and Lecomte, J. T. J. (2007) Structural and thermodynamic consequences of *b* heme binding for monomeric apoglobins and other apoproteins. *Gene* 398, 12–28.

(76) Nishimura, C., Lietzow, M. A., Dyson, H. J., and Wright, P. E. (2005) Sequence determinants of a protein folding pathway. *J. Mol. Biol.* 351, 383–392.

(77) Eun, Y.-J., Kurt, N., Sekhar, A., and Cavagnero, S. (2008) Thermodynamic and kinetic characterization of apoHmpH, a fast-folding bacterial globin. *J. Mol. Biol.* 376, 879–897.

(78) Zhu, L., Kurt, N., Choi, J., Lapidus, L. J., and Cavagnero, S. (2013) Sub-millisecond chain collapse of the *Escherichia coli* globin apoHmpH. *J. Phys. Chem. B* 117, 7868–7877.

(79) Codutti, L., Picotti, P., Marin, O., Dewilde, S., Fogolari, F., Corazza, A., Viglino, P., Moens, L., Esposito, G., and Fontana, A. (2009) Conformational stability of neuroglobin helix F—possible effects on the folding pathway within the globin family. *FEBS J.* 276, 5177–5190.

(80) Hargrove, M. S., Krzywda, S., Wilkinson, A. J., Dou, Y., Ikeda-Saito, M., and Olson, J. S. (1994) Stability of myoglobin: a model for the folding of heme proteins. *Biochemistry* 33, 11767–11775.

(81) Smith, L. P. (2003) Effects of Amino Acid Substitution on Apomyoglobin Stability, Folding Intermediates, and Holoprotein Expression. Ph.D. Thesis, Rice University, Houston.

(82) Samuel, P. P., Smith, L. P., Phillips, G. N., Jr., and Olson, J. S. (2015) Apoglobin stability is the major factor governing both cell-free and *in vivo* expression of holomyoglobin. *J. Biol. Chem.* 290, 23479–23495.

(83) Ferrer, J. C., Guillemette, J. G., Bogumil, R., Inglis, S. C., Smith, M., and Mauk, A. G. (1993) Identification of Lys79 as an iron ligand in one form of alkaline yeast iso-1-ferricytochrome *c*. *J. Am. Chem. Soc.* 115, 7507–7508.

(84) Rosell, F. I., Ferrer, J. C., and Mauk, A. G. (1998) Proton-linked protein conformational switching: Definition of the alkaline conformational transition of yeast iso-1-ferricytochrome *c*. *J. Am. Chem. Soc.* 120, 11234–11245.

(85) Nye, D. B., Preimesberger, M. R., Majumdar, A., and Lecomte, J. T. J. (2018) Histidine–lysine axial ligand switching in a hemoglobin: A role for heme propionates. *Biochemistry* 57, 631–644.

(86) Aono, S., Ohkubo, K., Matsuo, T., and Nakajima, H. (1998) Redox-controlled ligand exchange of the heme in the CO-sensing transcriptional activator CooA. *J. Biol. Chem.* 273, 25757–25764.

(87) Block, D. R., Lukat-Rodgers, G. S., Rodgers, K. R., Wilks, A., Bhakta, M. N., and Lansky, I. B. (2007) Identification of two heme-binding sites in the cytoplasmic heme-trafficking protein PhuS from *Pseudomonas aeruginosa* and their relevance to function. *Biochemistry* 46, 14391–14402.

(88) Tripathi, S., O'Neill, M. J., Wilks, A., and Poulos, T. L. (2013) Crystal structure of the *Pseudomonas aeruginosa* cytoplasmic heme binding protein, Apo-PhuS. *J. Inorg. Biochem.* 128, 131–136.

(89) Mukhopadhyay, K., and Lecomte, J. T. J. (2004) A relationship between heme binding and protein stability in cytochrome *b*₅. *Biochemistry* 43, 12227–12236.

(90) Robinson, C. R., Liu, Y., O'Brien, R., Sligar, S. G., and Sturtevant, J. M. (1998) A differential scanning calorimetric study of the thermal unfolding of apo- and holo-cytochrome *b*₅₆₂. *Protein Sci.* 7, 961–965.

(91) Scott, N. L., Xu, Y., Shen, G., Vuletich, D. A., Falzone, C. J., Li, Z., Ludwig, M., Pond, M. P., Preimesberger, M. R., Bryant, D. A., and Lecomte, J. T. J. (2010) Functional and structural characterization of the 2/2 hemoglobin from *Synechococcus* sp. PCC 7002. *Biochemistry* 49, 7000–7011.